Modelling and analysis of offshore energy systems on North Sea oil and gas platforms

Tuong-Van Nguyen[a,*], Brian Elmegaard[a], Leonardo Pierobon[a], Fredrik Haglind[a], Peter Breuhaus[b]

[a]*Section of Thermal Energy, Department of Mechanical Engineering, Technical University of Denmark,*
Building 403, Nils Koppels Allé, 2800 Kongens Lyngby, Denmark
[b]*Department of Energy, International Research Institute of Stavanger,*
Professor Olav Hanssens vei 15, 4021 Stavanger, Norway

Abstract

Offshore processes are associated with significant energy consumption and large CO_2 emissions. Conventional North Sea oil and gas facilities include the following operations: crude oil separation, gas compression and purification, wastewater treatment, gas lifting, seawater injection, oil and gas export, and power generation. In this paper, a generic model of a North Sea oil and gas platform is described and the most thermodynamically inefficient processes are identified by performing an exergy analysis. Models and simulations are built and run with the tools Aspen Plus®, DNA and Aspen HYSYS®. Results reveal that the total exergy destruction of the system is particularly sensitive to the gas-to-oil ratio and amounts to 55-65 MW, while the total exergy losses amount to 15-20 MW. The gas compression train and the production manifold module are the most exergy-destructive operations of the oil and gas processing system, consuming 4-6 MW and 3-7 MW respectively, while the power generation system alone is responsible for 54-63 MW.

Keywords: Modelling, Energy Systems, Exergy Analysis, Oil and Gas platforms

1. Introduction

North Sea oil and gas platforms were responsible for about 26% of the total gross CO_2 emissions of Norway in 2011 [1]. It is generally assumed that the energy intensity and environmental impact of these offshore facilities will increase in the coming years, as a direct consequence of larger energy use to enhance hydrocarbon production [2, 3].

Concerns exist about the possible ways of evaluating and increasing the performance of these operations and thus reducing their environmental footprint. Exergy analysis is a method based on the 2nd law of thermodynamics which has been widely used to characterise the efficiency of various industrial processes. Exergy is defined as the maximum theoretical useful work that can be extracted from any given system, in reference to a specific environment. Unlike energy, exergy can be destroyed; this enables locating and quantifying sources of thermodynamic irreversibilities. Exergy can also be interpreted as a quantification of primary energy and exergy destruction account thus for use of fuel throughout a process [4, 5].

Only a few studies have been conducted on the modelling and thermodynamic performance assessment of offshore platforms. Oliveira and Van Hombeeck [6] simulated a Brazilian petroleum plant with HYSIM and focused exclusively on the separation, compression and pumping modules. Their study showed that the most exergy-consuming steps were the petroleum heating operation taking place within the separation module, and the gas compression process. The separation step had the worst exergetic efficiency (22.2%) of the overall plant, which had by itself an exergetic efficiency of 9.7%. The authors suggested that the large exergy destruction taking place in the heating step was due to the high difference between the temperatures of the exhaust gases and of the petroleum, and that newer separation technologies could improve the thermodynamic performance of the platform.

Voldsund et al. [7, 8] simulated a specific North Sea offshore platform by using Aspen HYSYS®. The

---
*Principal corresponding author. Tel.: +4545254129
Email address: tungu@mek.dtu.dk (Tuong-Van Nguyen)

Nomenclature

Acronyms

DNA Dynamic Network Analysis

NHV Net Heating Value, kJ/kg

$NRTL$ Non-Random Two Liquid

Greek Letters

β chemical exergy correction factor

η efficiency

Latin Letters

$\bar{e}$ specific exergy (molar), J/mol

$\bar{R}$ ideal gas constant, J/(mol.K)

E exergy, J

e specific exergy (mass), J/kg

h specific enthalpy (mass), J/kg

s specific entropy (mass), J/(kg.K)

x partial pressure

z pollutant mass fraction

Subscripts and superscripts

$*$ relative

f fuel

p product

0 dead state

ch chemical

d destruction

kn kinetic

k component

l loss

ph physical

pt potential

---

platform investigated in their study included separation, recompression and reinjection trains as well as fuel gas and export pumping systems. Results showed that the largest exergy destruction occurred in the gas re-injection trains (44.4%) and in the recompression process (17%). The authors reported an overall exergetic efficiency of 32% in the baseline case and suggested that the thermodynamic losses of the platform could be greatly reduced by avoiding anti-surge recycling and using more efficient compressors [8]. However, these previous studies considered specific inflow conditions and focused on the oil processing plant exclusively. The impacts of variations in production flows have not been thoroughly estimated and the utility systems for heat and power generation have not been assessed.

The present paper aims, on the one hand, to introduce models describing the full- and part-load behaviour of typical offshore platforms, which include the processing plant and the utility sub-systems. On the other hand, it attemps to assess the thermodynamic performance of the complete system and to quantify the effects of variations in the well-fluid composition. A generic process model of a North Sea oil platform is thus presented and analysed with respect to the 2nd law of thermodynamics. In contrast to the previous works undertaken within this field, the production manifolds, the glycol dehydration and wastewater treatment processes, as well as the power generation systems with their part-load characteristics, are considered and analysed.

2. System description

Petroleum by itself is relatively dry and has a low content of light hydrocarbons, but is extracted along with gas and water. Offshore separation of these three phases is required to maximise the oil production and to minimise its gas and water content, for economical and process requirement issues. Crude oil is shipped onshore, while gas and water are either valorised or rejected into the environment. Factors such as the well-fluid thermo-physical properties, chemical composition, gas-to-oil (GOR) and water-to-oil (WOR) ratios, reservoir properties (e.g temperature, pressure, permeability) may strongly differ from one field to another, which implies that different technical considerations (e.g pressure and temperature levels) and technological choices (e.g number of trains, gas export, system configuration) apply for different cases. In addition, production flows vary significantly with time, affecting the plant performance [2].

However, although design differences exist amongst various North Sea oil platforms, it is worth noticing that gas purification and exportation, waste water treatment and seawater injection, have become the most preferred gas and water processing routes in this region [3]. Since the North Sea crude oil and natural gas are characterised by a low content of salt, hydrogen sulphide and carbon dioxide, neither desalting nor sweetening units are necessary. Typical offshore processing on North Sea oil platforms consists of 8 different sub-systems, namely:

- Production manifolds

- Crude oil separation

- Oil pumping and export

- Gas re-compression and purification

- Gas compression – lifting and exportation –

- Wastewater treatment

- Seawater injection

- Power generation

Hence, the generic platform model developed within this study includes the aforementioned processes and is based on the system configurations presented in the open literature for the crude oil processing [3, 9–12], for the gas treatment process [11–13], and for the water processing [14, 15]. A conceptual layout of the platform model, illustrating schematically material flows and interactions between the various parts of the plant, is shown in Figure 1. Internal system configurations, such as condensate recycling and anti-surge control, are not shown but are considered in the system modelling.

3. System modelling and simulation

3.1. System inputs

Crude oil contains a large inventory of multiple chemical compounds such as alkanes, alcenes and aromatics, ranging from light to heavy, branched to cyclic and saturated to unsaturated hydrocarbons. Complete compositional analyses are rarely carried out, which implies that the exact chemical composition of crude oil – nature of chemical compounds and amounts – is usually unknown. In general, crude oil is characterised by conducting a true boiling point

(TBP) analysis: crude oil is separated into distillate fractions with different hydrocarbons composition and boiling points. The distribution of the boiling point range as a function of the fraction of crude oil distilled is called the true boiling point curve and gives an approximation of the crude oil properties and composition. Molecular weight, viscosity, specific density and gravity are measured for each distillate fraction, and thermal properties such as heating value and thermal conductivity are estimated by empirical correlations [9, 16].

Hence, it is not possible to define crude oil as an exact mixture of known components with known proportions. Crude oil is therefore represented by a group of known and hypothetical (also denominated pseudo-) components whose properties are created from the true boiling curve [9, 16]. In this study, crude oil is modelled as a mixture of 83 chemical compounds: CO_2, H_2O, O_2, N_2, Ar, H_2S, 47 hydrocarbons and 29 pseudo-components. Bulk properties of the crude oil mixture are given in Table 1.

Table 1: Crude oil properties

	Crude Oil
API	39.9
Specific gravity	0.826
Density (kg.m^{-3})	825.5
Light ends cut ($\%_{vol}$)	27.2

Gas may either be mixed with oil and enter the platform system through the same wells (associated gas) or be processed apart through specific wells (non-associated gas). In this paper, only associated gas was considered since it is the most encountered case in oil offshore processing, according to Bothamley et al. [3]. As seen in Table 2, North Sea natural gas has a low content of hydrogen sulphide and carbon dioxide, which justifies its appellation of sweet gas.

Table 2: Associated natural gas composition

Chemical Compound ($\%_{mol}$)	Natural Gas
N_2	4.37
CO_2	1.34
H_2S	0.2
CH_4	73.7
C_2H_6	6.10
C_3H_8	6.70
n-C_4H_{10}	2.48
i-C_4H_{10}	1.41
C_5+	3.70

Standard air, with a molar composition of 77.29% N_2, 20.75% O_2, 1.01% H_2O, 0.92% Ar and 0.03% CO_2, and standard seawater are processed in the offshore platform.
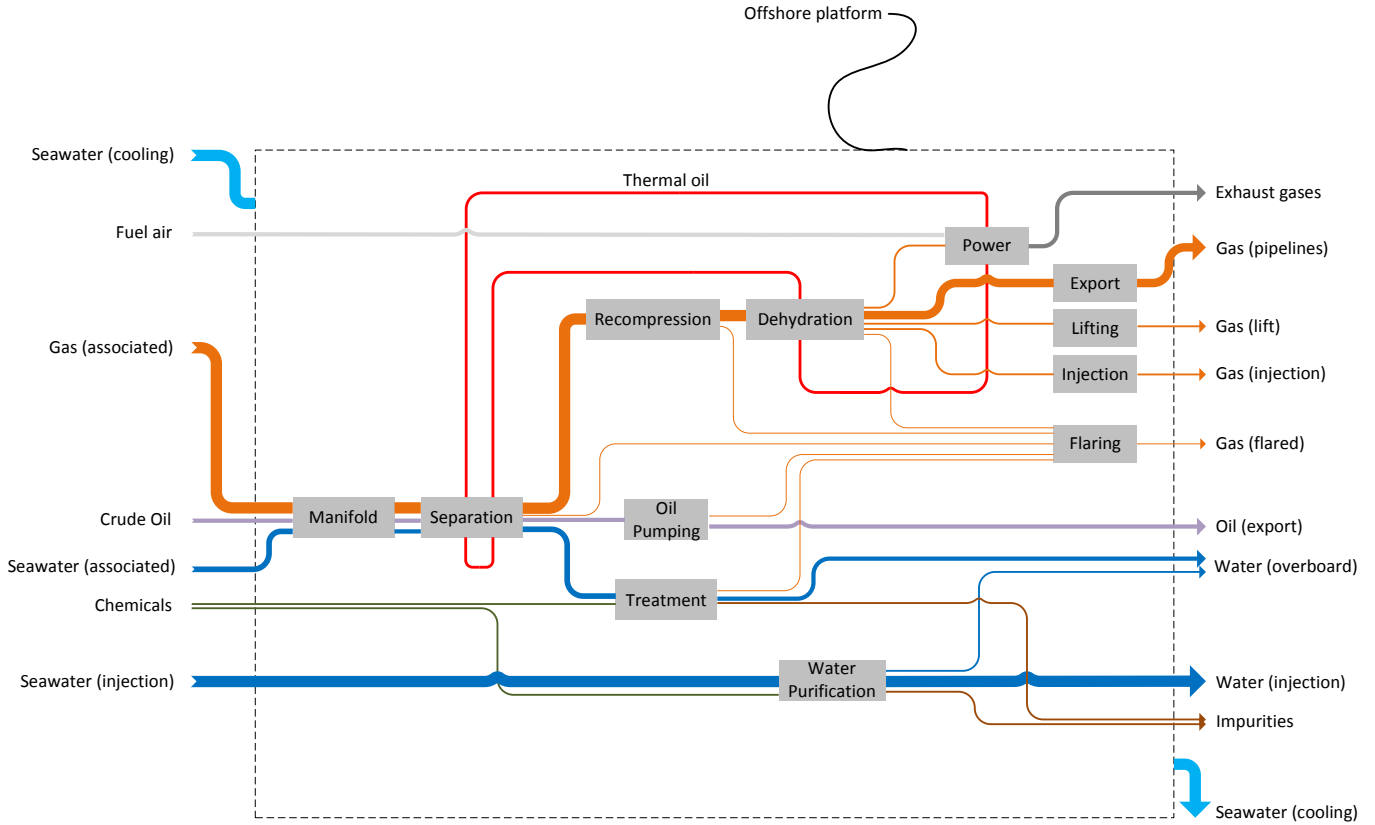
Figure 1: Conceptual layout of offshore processes on North Sea oil platforms

3.2. System sub-models

The overall platform system was divided into sub-systems which were at first modelled separately and integrated afterwards in an overall model. The main aim of this system decomposition into sub-models was to investigate the steady-state behaviour of each process, to evaluate their thermodynamic performances and their sensitivity to operating parameters. Sub-systems and corresponding mathematical models created within this study are described in the following sections. Unless something else is stated, operating parameters of each process model are fixed by the user and the models return the energy demand as well as the flow rates and compositions of the material streams. Modelling and simulation assumptions are presented in Table 3. Values in brackets [-] indicate several components of the specified type, each value corresponding to a particular component at a given location in the process.

Simulations based on case studies available in the open literature [6–8, 11, 12] were performed to validate the separation, gas re-compression and injection process models and showed a deviation smaller than 5%. The maximum difference is found in the pre-

diction of the gas volumic flowrate at the outlet of the offshore platform system. Comparisons between manufacturer data and model predictions were conducted to validate the models developed for simulating the behaviour of the power generation units. For loads above 50%, which is the region of interest, the maximum relative error is found in the prediction of the gas turbine thermal efficiency and is around 3.7%.

3.2.1. Crude oil processing

Petroleum extracted through the several wells is transferred to the platform complex via a network of pipelines and a system of production manifolds. The individual well-streams are mixed and de-pressurised by choke boxes, which consist of valves and chokes, and fed afterwards into the separation train. Crude oil separation is promoted by gravity and takes place in four stages operating at four different pressure levels. The first three stages consist of three- and two-phase separators while the last stage comprises an electrostatic coalescer [3, 11, 12].

Pressure is decreased along the train by a series of throttling valves and the temperature of the separator feeds is increased by heat exchange with thermal oil

Table 3: General system specifications

| Process	Component	Parameter	Unit	Value
Reservoir		Temperature	°C	71
		Pressure	MPa	7
Production Manifold	Throttle	Outlet pressure	MPa	[12,7]
	Mixer	Pressure drop	MPa	0.12
Separation	3-Phase Separator	Heat losses	MW	-
		Pressure level	MPa	[7,2.9,0.72]
		Pressure drop	bar	[0.5,0.3,0.05]
	Electrostatic coalescer	Heat losses	MW	-
		Pressure level	MPa	0.18
	Mixer	Pressure drop	bar	[0.05,0.02]
	Crude oil/glycol heat exchanger	Pressure drop	bar	[0.25,0.25]
		Temperature increase (cold side)	K	5
		Minimum temperature approach	K	10
Re-compression	Centrifugal compressor	Outlet pressure	MPa	[2.95,7]
		Isentropic efficiency	%	[64,67]
		Mechanical efficiency	%	[93,93]
	Gas/seawater heat exchanger	Outlet temperature	°C	[20,20,20]
		Pressure drop	bar	[0.25,0.1,0.025]
	Throttle	Outlet pressure	MPa	[2.93,0.75,0.18]
	Flash	Heat losses	MW	-
		Pressure drop	bar	[0.5,0.3,0.05]
Oil pumping	Pump	Outlet pressure	MPa	[0.545;3]
		Pump efficiency	%	[59,61]
		Driver efficiency	%	[90,90]
	Cooler	Outlet temperature	°C	15
		Pressure drop	bar	0.1
Waste water treatment	Throttle	Outlet pressure	MPa	0.12
	Cooler	Outlet temperature	°C	[25,15]
		Pressure drop	bar	[0.1,0.1]
	Hydro-cyclone	Separation Efficiency	%	97
	Skim vessel	Pressure level	bar	1.2
		Temperature level	°C	25
Glycol dehydration	Absorption column	Pressure level	MPa	7
		Temperature level	°C	31
		Minimum glycol-gas temperature approach	°C	18.5
	Flash drum	Temperature level	°C	37.8
	Throttle	Outlet pressure	bar	1.2
	Glycol/Thermal oil heat exchanger	Outlet temperature (cold side)	°C	165
		Pressure drop	bar	0.025
	Glycol/Seawater heat exchanger	Outlet temperature (hot side)		
		Pressure drop	bar	0.025
	Desorption column	Number of stages	-	5
		Stage efficiency	-	100%
		Condenser pressure	bar	1.2
		Condenser pressure drop	bar	0.2
		Condenser temperature	°C	98.9
		Reboiler pressure	bar	1.25
		Reboiler pressure drop	bar	0.2
		Reboiler temperature	°C	204.4
Waste heat recovery system		Temperature level (glycol side)	°C	[200,210,220]
Seawater injection system		Oxygen level	ppb	10
		Solids content	ppm	5
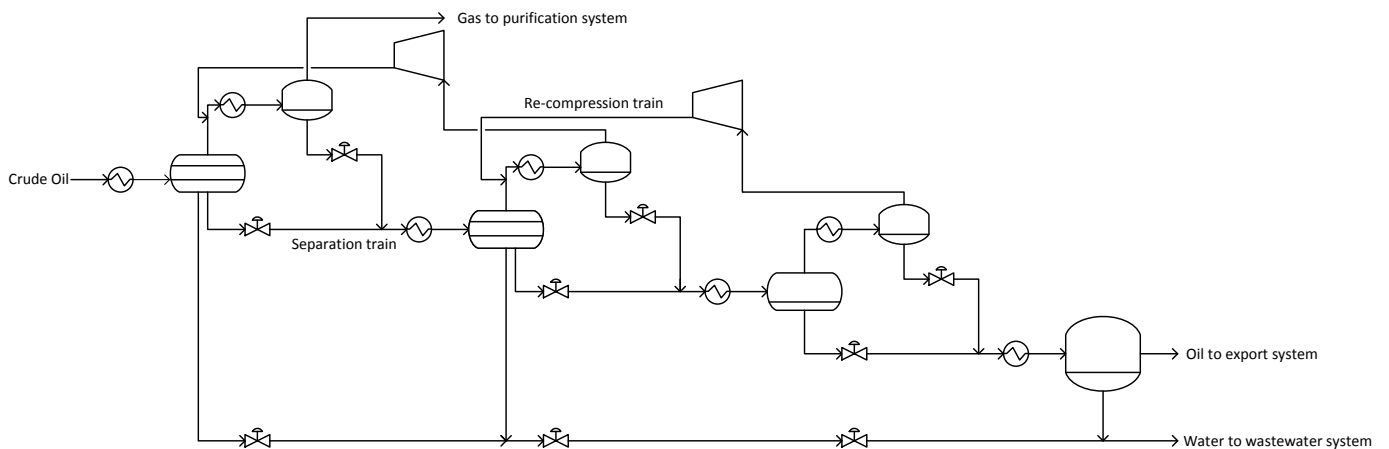
Figure 2: Flow sheet of the separation and gas re-compression train
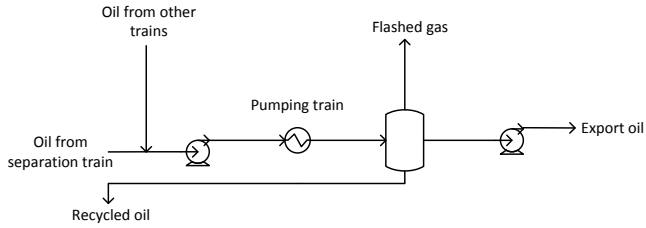
Figure 3: Flow sheet of the export pumping section

Figure 4: Flow sheet of the dehydration train

to increase the separation efficiency, as depicted in Figure 2. It is assumed that the gravity separators are continuously operated, that physical equilibrium is reached and that no liquid is entrained in the gas vapour phase. Power needed to sustain the electric field in the coalescer is neglected.

3.2.2. Gas re-compression

Product gas from the separators and recovered from the oil pumping train is led through the re-compression train. Temperature is decreased by seawater cooling and liquid droplets are separated and removed by scrubbing, resulting in a relatively dry gas which is then re-compressed. Condensate from the scrubbers is mixed with crude oil at the inlet of the separators, while pressurised gas is sent to the purification process. It is assumed that the gas re-compressors are run at a sufficient load, close to their design point, which avoids the need for recycling around these components to prevent surge issues.

3.2.3. Oil export and pumping

Oil from the separation train enters the export pumping system, shown in Figure 3, where it is mixed with oil and condensate removed in other steps of the plant. It is then cooled, pumped gradually, stored and exported to the coast via shipping.

3.2.4. Gas purification

In addition to the re-compression train, there are needs for a dehydration unit to prevent corrosion issues in gas pipelines, as illustrated in Figure 4, and for additional flash units to reduce the content of heavy hydrocarbons. Gas dehydration on offshore platforms is conventionally achieved by a glycol absorption/desorption system. Wet gas enters at the bottom of an absorption column, modelled as a packed absorber, and water is captured by liquid glycol by physical absorption. The glycol-water-natural gas mixture thereby enters a flash separator at an intermediate pressure to minimise the amount of nat-
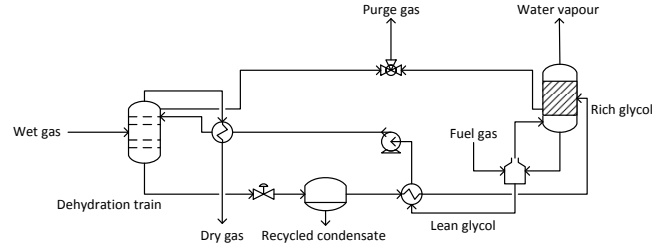
ural gas entrained with the circulating glycol. It is then pre-heated to ease the water-glycol separation in the desorption column. A small fraction of dry natural gas is sent for stripping in order to increase the molar purity of glycol to 99.9%. Regenerated glycol is pumped to the absorber pressure and heated to ensure a minimum temperature difference of 20°C with the natural gas stream entering the system [12, 16, 17].

In contrast of the other process sub-models, in which operating parameters and inflows were set by the user or returned by other sub-models, and outflows derived by mass and energy balances, the gas dehydration sub-model calculates the optimal operating parameters (glycol and stripping gas flow rates, boilup and reflux ratios, heating demand) for a set of given constraints (water content, temperature level) on the outflows. The gas purification sub-model calculates the amount of circulating glycol required to reach a purity of 99.9% of natural gas at the outlet of the dehydration unit as well as the stripping gas flowrate.

3.2.5. Wastewater treatment

In the North Sea region, downstream cleaning of the produced water is essential for environmental and legislation reasons [18]: suspended particulates and dissolved hydrocarbons are removed by use of hydrocyclones. Wastewater flows then through a succession of throttles and enters a skimmer tank to recover oil traces before it is released to the environment.

3.2.6. Seawater injection

Seawater for re-injection must meet several quality requirements to avoid pipe corrosion and bacteria formation due to sediments, sulphides and oxygen compounds [19, 20]. It is processed in filtering units and deaeration towers before being pumped and injected into the petroleum reservoir. The seawater injection model calculates the chlorine and coagulants loading

required to decrease the concentration of oxygen and particulates to the desired level. It is at first assumed that the volume of water which should be injected into the reservoir is nearly constant. The impact of this assumption is evaluated later within this study by means of a sensitivity analysis.

3.2.7. Gas compression, lifting and exportation

A first fraction of the dry gas is used for lifting, which consists of injecting gas at high pressure into the reservoir via the oil wells to increase crude oil recovery. Lifting gas is cooled and scrubbed to further remove heavy hydrocarbons and to decrease the power requirements of the compressors. A second fraction of the dry gas is also cooled and compressed before being sent onshore through a network of subsea pipelines.

3.2.8. Power generation utility system

Electric power required at the different process modules is usually produced by gas turbines directly running on-site. They are selected considering the maximum expected power requirements over the offshore facility's life cycle. However, for reliability matters and in order to prevent unexpected plant shutdown, power generation is usually shared amongst multiple gas turbines running at part-load, which implies that their maximum thermal efficiency is not reached. In this study, the power utility system is modelled as two twin-spool gas turbines complemented by power turbines sharing equally the electrical power supply, with characteristics based on the SGT-500 engine developed by SIEMENS [21]. As shown in Figure 5, the gas turbine is connected to a waste heat recovery system: the thermal fluid is assumed to be a glycol/water mixture with a mass ratio of 40/60.
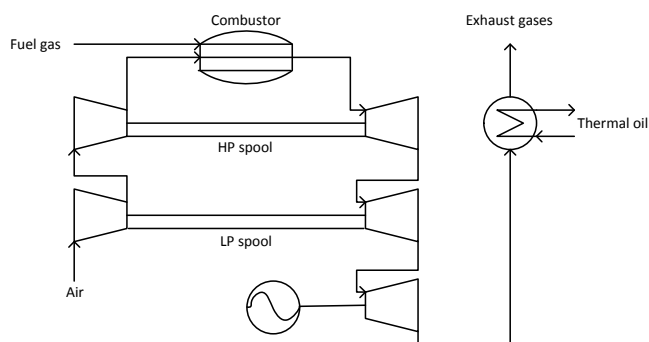

Figure 5: Flow sheet of the twin-spool gas turbine system

The developed power generation sub-model takes as input the electrical power demand from the other plant sections and derives the compressor and turbine off-load characteristics by application of a stage-stacking analysis [22–24]. Air and gas flows, operating conditions and isentropic efficiencies of the gas turbine components are calculated for the required load and are returned to the waste heat recovery sub-model.

3.2.9. Heating and cooling utility systems

Heating on-site is ensured by the waste heat recovery system connected to the gas turbines. In general, the highest temperature level of the platform is found at the reboiler of the desorption column [3]. The waste heat recovery sub-model is based on the heating demand from the platform processes. It is used to calculate the stack temperature of the exhaust flue gases of the power generation system, based on the assumption that the temperature of the thermal fluid is $200°C$ and $220°C$ at the inlet and outlet of the waste heat recovery system.

Cooling water is utilised to decrease the amount of heavy hydrocarbons entrained with natural gas and to prevent foaming and low loads in the separation system. This system sub-model is based on the cooling demand of the separation and gas processing trains, and returns the required flow rate of seawater used for cooling. The rejection temperature to the environment is constrained to a maximum of $25°C$.

3.3. System simulation

3.3.1. Simulation basis

All processes, at the exception of the power generation and glycol dehydration processes, were simulated with Aspen Plus® version 7.2 [25]. Simulations of production manifolds, petroleum separation, oil pumping, gas re-compression, flaring and lifting were based on the Peng-Robinson equation of state, while simulations of the water purification and injection processes were based on the Non-Random Two Liquid (NRTL) model, usually more suited for electrolyte system modelling. Glycol dehydration was simulated with Aspen HYSYS® [26], using the glycol property package, claimed to predict more accurately the behaviour the tri-ethylene glycol-water mixture [17, 27]. Power generation was simulated by using the tool Dynamic Network Analysis (DNA), developed at the Technical University of Denmark [28].

3.3.2. Case studies and sensitivity analysis

Three cases have been investigated within this study, corresponding to the same platform – identical processes and operating conditions – but with different well-fluid compositions and loads. Specifications for each simulation are listed in Table 4. As emphasised by Svalheim et al. [2], production flows are strongly time-dependent. It is thus unlikely to find, for the same platform, three distinct situations with sensibly similar flow rates and sensibly different gas-to-oil (GOR) and water-to-oil (WOR) ratios. However, in order to provide a basis for comparison and to assess the impact of the gas and water contents of the well-fluid, each simulation case is defined on the same well-fluid molar flow rate.

Case 1, referred as the baseline case in the rest of this study, aims to represent a regular operation of an offshore platform, with oil, gas and water extracted along. Gas- and water-to-oil ratios have been chosen based on the production data of different oil platforms operating in the North Sea [29]. In the second case, the water-to-oil ratio is reduced by 50%, in order to describe the early life of an oil field, when only a small amount of water enters the platform system. Finally, the last case (Case 3) is featured by the same water-to-oil ratio as in the baseline case, but the gas molar fraction is increased by 33%, which corresponds to an intermediate situation in the lifespan of an oil field.

Table 4: Simulation specifications

Well-fluid properties		Case 1	Case 2	Case 3
Molar flow rate	(kmol/hr)	18446	18446	18446
Associated gas	%	48.60	50.71	64.80
Associated water	%	42.90	27.34	17.47
Crude oil	%	8.45	10.76	3.44
Gas-to-oil ratio	molar	5.75	4.71	18.85
Water-to-oil ratio	molar	5.08	2.54	5.08
Mass flow rate	(10^3 kg/hr)	618.3	696.5	490.8
Actual volume flow rate	(m^3/hr)	1484	1841	2079

Operating parameters such as seawater flow rate and gas export pressure differ from platform to platform depending on the physical properties of the oil field and on the pipeline network requirements. These design set-ups are varied one-at-a-time: default states set in the baseline cases and variation ranges in this parametric study are shown in Table 5.

Table 5: Sensitivity analysis parameters

Parameter	Unit	Default value	Variation range
Seawater injection flowrate	(Sm^3/hr)	1245.3	[900-2900]
Gas export pressure	(MPa)	17	[15-25]

4. Exergy analysis

4.1. Exergy balance

The concept of exergy derives from both the 1st and 2nd laws of thermodynamics and illustrates the potential of a system to bring change to its environment. Unlike energy, exergy is not conserved in non-ideal processes, which, in other words, means that the exergy entering a system is always larger than the exergy exiting it. The difference between the inlet $\dot{E}_i$ and outlet exergy $\dot{E}_o$ flow rates is called the exergy destruction rate $\dot{E}_d$, which indicates thus the locations and amplitudes of energy degradation [4]. The general exergy balance for a given system at steady-state can be expressed as follows:

$$\dot{E}_d = \sum \dot{E}_i - \sum \dot{E}_o \tag{1}$$

For a control volume at steady state, the exergy destruction rate becomes:

$$\dot{E}_d = \sum \left(1 - \frac{T_0}{T_j}\right) \dot{Q}_j - \dot{W}_{cv} + \sum \dot{m}_i e_i - \sum \dot{m}_e e_e \tag{2}$$

Where e and $\dot{m}$ are the specific exergy and mass flow rate of a material stream, respectively, and $\dot{Q}_j$ and $\dot{W}_{cv}$ the time rates of energy transfer by heat and work. The subscript 0 indicates the reference conditions, the subscripts i and e denote inlet and exit and the subscript j the boundary of the component of interest.

4.2. Exergy components

Alike enthalpy and entropy, exergy is an extensive property which can be defined for every stream of matter. The specific exergy of a material stream e is a function of its physical e_{ph}, chemical e_{ch}, kinetic e_{kn} and potential e_{pt} components and is defined as:

$$e = e_{ph} + e_{ch} + e_{kn} + e_{pt} \tag{3}$$

In this study, the kinetic and potential effects on the exergy associated with material streams are assumed negligible compared to the physical and chemical contributions. Physical exergy is related to temperature and pressure differences with the dead state, while chemical exergy is related to deviations in chemical composition with reference substances

present in the environment. The specific physical exergy per mass of a given stream e_{ph} can be calculated with the following formula:

$$e_{ph} = (h - h_0) - T_0(s - s_0) \quad (4)$$

Where h and s are the specific enthalpy and entropy of a stream of matter per unit-of-mass, respectively. By applying the Peng-Robinson and Non-Random-Two-Liquid thermodynamic equations of states, physical exergy values can be computed and deduced from the process simulations. Values of chemical exergy for pure substances are extracted from the reference models of Szargut and Morris [30, 31]. Chemical exergy of hypothetical components contained in crude oil is calculated with the following formula from Rivero [32] when their chemical composition is approximatively known:

$$E_{ch,i} = \beta NHV_i + \sum z_j E_{ch,j} \quad (5)$$

Where NHV_i stands for the Net Heating Value, z_j the mass fraction of metal impurities, $E_{ch,j}$ the corresponding chemical exergy and β the chemical exergy correction factor, expressed as:

$$\beta = 1.0401 + 0.1728\frac{z_{H_2}}{z_C} + 0.0432z_{O_2}z_C +$$
$$0.2169z_S z_C + (1 - 2.0628z_{H_2}z_C) + 0.0428\frac{z_{N_2}}{z_C} \quad (6)$$

In the case that the chemical structure of an hypothetical component is unknown, the following relation is used, and gives, according to Rivero [32], less than 1% deviation:

$$E_{ch,i} = NHV_i \quad (7)$$

Finally, the specific chemical exergy of a mixture $\bar{e}_{ch,mix}$, on a molar basis, becomes:

$$\bar{e}_{ch,mix} = \sum x_k \bar{e}_{ch,k} + \bar{R}T_0 \sum x_k ln(x_k) \quad (8)$$

Where x_k is the partial pressure of the k gas and $\bar{R}$ the ideal gas constant.

4.3. Exergy efficiency

Applying an exergy balance on a specific process component k and calculating its exergy destruction rate $\dot{E}_{d,k}$, provides information on its thermodynamic inefficiencies. The exergy destruction rate of this component can then be related to the exergy destruction rate of the whole system $\dot{E}_d$ by calculating the exergy destruction ratio y_k^*, defined as:

$$y_k^* = \frac{\dot{E}_{d,k}}{\dot{E}_d} \quad (9)$$

Exergetic efficiency η_k for a sub-system k, which is a measure of its thermodynamic performance, can be defined by identifying fuel and product of interest. It should be emphasised that fuel and product exergies $\dot{E}_{f,k}$ and $\dot{E}_{p,k}$ of the sub-system of interest are not necessarily equal to its input $\dot{E}_{i,k}$ and output exergies $\dot{E}_{o,k}$.

$$\eta_k = \frac{\dot{E}_{p,k}}{\dot{E}_{f,k}} \quad (10)$$

Definitions of exergetic fuels and products for the components and sub-systems investigated within this study are extensively discussed in Bejan et al [4] and in Kotas [5].

5. Results

5.1. System simulation

This section introduces and discusses the results of the oil offshore platform modelling, which was described in detail in Section 3. Results of the process plant simulation are presented in Table 6, with flows expressed in standard cubic meters (Sm^3), which stands for volume measurements in standard conditions (temperature of 15°C and pressure of 1 atm). The power requirements of the offshore platform are shown in Table 7, with values expressed in MW.

Table 6: Processing plant simulation results - Outflow streams

System outputs		Case 1	Case 2	Case 3
Gas (export)	$(10^3 \ Sm^3/hr)$	166.4	213.4	279.4
Gas (lift)	$(10^3 \ Sm^3/hr)$	24.36	31.24	40.89
Water (overboard)	(Sm^3/hr)	123.3	90.00	50.41
Water (injected)	(Sm^3/hr)	1245	1245	1245
Oil (export)	(Sm^3/hr)	359.2	457.4	156.3

Results indicate that the power consumption of the offshore platform ranges from 18 to 23.5 MW and is strongly correlated to the energy demand of the gas lifting and exportation trains. In any case, this specific process is the major electricity consumer of the offshore plant and is responsible for 50% to 65% of the total power demand. This power consumption, both in absolute and specific terms, is larger in case 3 than in cases 1 and 2, as the power required to compress

Table 7: Processing plant simulation results – Power consumption (MW)

Power consumption	Case 1	Case 2	Case 3
Gas lifting and exportation	9.234	11.95	15.09
Seawater injection	6.973	6.973	6.973
Gas recompression	1.234	2.132	1.111
Oil pumping	0.530	0.674	0.230
Glycol dehydration	0.004	0.005	0.005
Wastewater treatment	-	-	-
Total (MW)	17.98	21.30	23.41
Total (MJ/Sm^{3}oil)	180.2	167.6	539.2
Total (MJ/Sm^{3}oil,eq)	117.7	109.2	176.8

the surplus of gas overcomes the decrease of power in the crude oil pumping and wastewater treatment sections. Additionally, gas compressors on offshore platforms are characterised by a relatively low isentropic efficiency and the use of anti-surge gas recycling has also an impact on the train power consumption.

Another important aspect of the power consumption profile of oil offshore platforms is the great demand associated with the seawater injection process, as a large amount of seawater must be pumped from atmospheric pressure to 11.5 MPa. This process demand accounts for 29% to 39% of the total power consumption and reaches nearly 7 MW. Seawater pumped for injection is not extracted through the same wells as oil and natural gas and does not enter the crude oil separation train. Conversely, oil, associated water and gas do thus not enter the water purification train, and variations in the well-fluid composition do therefore not directly affect the pumping work for seawater injection.

The third largest power demand of the offshore facility is the gas re-compression process, in which gaseous streams from the two- and three-phase separators are re-compressed to the original pressure level of 7 MPa. The electrical energy consumption of this system is larger by a factor two in the second case than in the first one, due to the larger fraction of crude oil and associated gas in the well-stream entering the separation train. Consequently, a greater amount of gas is recovered in the separation train and flows through the two booster compressors. However, although the associated gas flow rate is larger in case 3 than in case 2, the power demand of the re-compression train is much smaller, which suggests that most of the associated gas, rich in light-weight hydrocarbons, exits the separation train at the first separator and bypasses the booster compressors. In other words, the gas recompression power consumption is mostly dependent on the crude oil flow rate

and composition, which contains medium-weight hydrocarbons such as propane and butane, more likely to vaporise in the second and third stages of the separation process.

In contrast, the variations of the associated water and oil flows in cases 2 and 3 have a limited impact on the process plant power consumption, because the oil pumping and water treatment processes have by themselves a low power demand. The power consumption of the dehydration unit is slightly higher in the case 3. As a result of a larger gas flow rate at the outlet of the recompression train, a greater amount of tri-ethylene must be processed to decrease the water content to the same purity level. However, as the main natural gas stream only flows through the absorption unit, electricity required by this process is only needed to compensate the pressure drops in the desorber column and to pump the liquid glycol from the desorber to the absorber pressure.

Table 8: Utility system simulation results – Characteristics (for 1 twin-spool turbine)

		Case 1	Case 2	Case 3
Air	Gas turbine inlet			
$\dot{m}$	(kg/s)	75.5	78.1	82.9
Gas	Combustion chamber inlet			
$\dot{m}$	(kg/s)	0.73	0.78	0.87
T	(°C)	15	15	15
P	(bar)	10.8	10.8	10.8
Flue Gases	Gas turbine outlet			
$\dot{m}$	(kg/s)	76.2	78.9	83.7
T	(°C)	316.1	324.6	330.6
P	(bar)	1.02	1.02	1.02
Flue Gases	Waste heat recovery outlet			
T	(°C)	266.9	277.6	286.3

5.2. Sensitivity analysis

The total power consumption of the oil and gas processing plant is, as seen in Table 7, strongly dependent on the power demands of the gas compression system and of the seawater injection process. Correlation between seawater volume and injection system power consumption is shown in Figure 6. Power consumption of the seawater injection train varies linearly with the volume of seawater to inject in the reservoir and increases by about 1 MW for each increment of 200 Sm^3/hr.

This result suggests that, as time goes on, since a larger seawater volume must be injected into the oil reservoir and a lower volume of gas is extracted, the power consumption of the water injection train may exceed the power demand of the gas compression process.
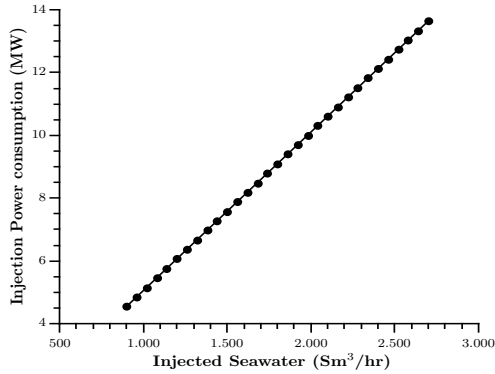
Figure 6: Effect of seawater injected volume on injection system power consumption

The gas export pressure is a parameter fixed by the requirements of the pipeline network system – since this value is subject to variations depending on the network and pipelines to which the offshore platform is connected, the effect of different pipeline constraints is illustrated in Figure 7. It is observed that the total compression train power consumption is clearly affected by the pressure level at which gas must be compressed. However, it is more likely that the operating pressure of the pipeline network system is between 18 and 22 MPa, which corresponds to a window of around 20% of the power demand of this process.
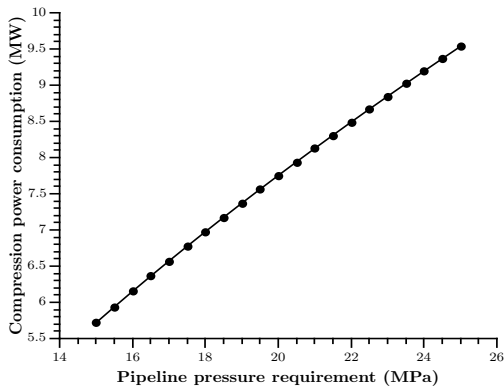

Figure 7: Effect of pipeline pressure requirement on compression train power consumption

5.3. Exergy analysis

In this study, an exergy analysis was undertaken based on dead state conditions of 5°C and 1 atmosphere. Exergy associated with each stream of matter present in the system is calculated and exergy destruction rates are examined for the three simulation cases. Based on the exergy analysis results calcu-

lated from the process simulation results, a simplified Grassmann diagram of the overall offshore platform system, which illustrates the input and output exergy flows for the baseline case, is shown in Figure 8.

Exergy is introduced in the form of raw materials (crude oil, associated gas and water, fuel air, seawater, chemicals) and exits in the form of valuable products (e.g crude oil and gas sent onshore) and waste streams (e.g wastewater and exhaust gases). The Grassmann diagram shows that the input and output exergies of this system are largely dominated by the exergy associated to the crude oil and gas streams, because of their high chemical exergy content. In the baseline case, the chemical exergy content of crude oil and gas are respectively 44.6 and 46.3 MJ/kg, and the exergies of these two materials are responsible for nearly 97% of the total exergy input. In comparison, the main contributors to exergy losses are material streams rejected to the environment without any practical use, such as flared gases, discharged seawater, wastewater and exhaust gases from the gas turbine systems, which represent in total less than 1%. Exergy associated with lifted gas and injected water is not considered as a loss, since these streams provide the benefit of increasing oil recovery. The exergy destruction rate accounts for about 1.3% of the total exergy input of the overall platform system: contributions of each sub-system are given in Table 9 for the three simulation cases and the distribution of the total exergy destruction over the various sub-systems is illustrated in Figure 9.

Results demonstrate that the total destroyed exergy on the overall offshore platform totals from 54.8 to 63.3 MW, with a share of 65-70% for the utility system (gas turbines and waste heat recovery) and 30-35% for the oil and gas processing system. This analysis shows that, although the production flows are significantly different from case to case, most of the total exergy destruction takes place within the power generation system, because of the large thermodynamic irreversibilities associated with chemical reactions occurring in the combustors.

When considering exclusively the oil and gas process plant, it is observed that the total exergy destruction of the latter is comprised between 15.5 and 19.1 MW. The exergy destruction within the production manifolds (3.05-7.18 MW) is particularly high, due to the pressure decrease from 16.5 to 7 MPa without generation of any useful product. Conversely, the exergy destruction within the gas compression and

Seawater for cooling (~0.1-0.2%) Chemicals (<0.2%) Fuel air (<0.1%) Exhaust gases (~0.3%) Flared gases (<0.1%)

Associated Gas Crude Oil Offshore platform Gas (~31.8%) Crude Oil (~60.5%)

Associated Seawater Seawater for Injection (~0.2-0.3%) Seawater to Overboard (~0.1-0.2%) Seawater for injection (~1.5%) Lift Gas (~4.5%)
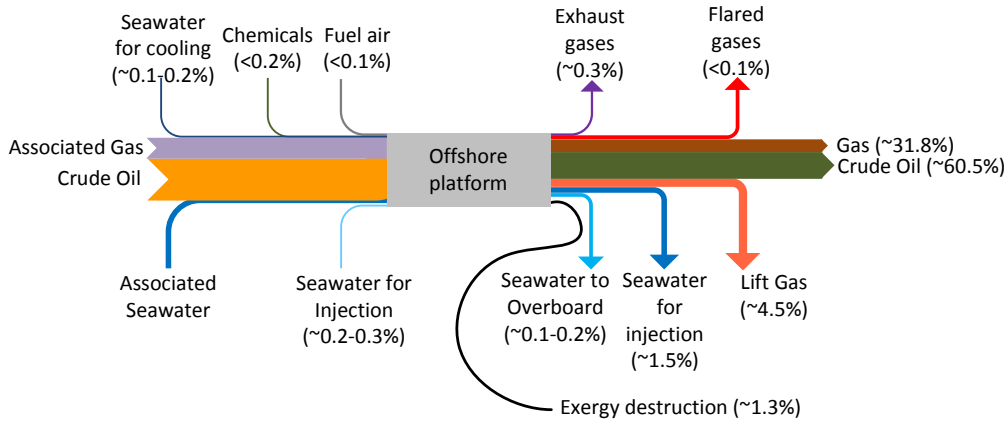
Exergy destruction (~1.3%)

Figure 8: Grassmann diagram of the offshore oil and gas platform – Baseline Case

Table 9: Exergy destruction rates (MW) of the analysed simulation cases for an oil offshore platform

	Case 1	Case 2	Case 3
Production manifold	**4.61**	**3.05**	**7.18**
Separation	**2.22**	**2.83**	**1.39**
Heaters	0.95	1.12	0.72
Throttles	1.02	1.33	0.51
Separators	0.11	0.17	0.07
Mixers	0.14	0.21	0.09
Recompression	**2.31**	**2.13**	**2.09**
Coolers	1.36	1.15	1.39
Throttles	0.29	0.08	0.12
Compressors	0.42	0.66	0.35
Mixers	0.18	0.18	0.18
Flashes	0.06	0.06	0.06
Wastewater	**0.49**	**0.17**	**0.09**
Gas compression	**4.17**	**5.20**	**6.39**
Compressors	3.74	4.56	5.59
Coolers	0.39	0.60	0.76
Throttles	0.02	0.02	0.02
Mixers	0.02	0.02	0.02
Glycol dehydration	**0.01**	**0.01**	**0.01**
Oil pumping	**0.26**	**0.23**	**0.07**
Seawater	**1.92**	**1.92**	**1.92**
Processing plant	**16.0**	**15.5**	**19.1**
Waste heat recovery	**2.85**	**2.96**	**3.15**
Power generation	**36.0**	**39.0**	**41.0**
Compressors	3.18	3.51	3.76
Combustion chamber	28.0	30.4	32.0
Turbines	4.80	5.07	5.24
Utility plant	**38.8**	**42.0**	**44.2**
Offshore platform	**54.8**	**57.5**	**63.3**
Total (MJ/Sm^{3}oil)	**549**	**452**	**1458**
Total (MJ/Sm^{3}oil,eq)	**359**	**295**	**478**

Exergy destruction share y_k^* (%)

Case 1 Case 2 Case 3

Production manifold Separation Gas recompression Wastewater treatment Gas exportation and lifting Dehydration Oil pumping Seawater injection Waste heat recovery Power generation
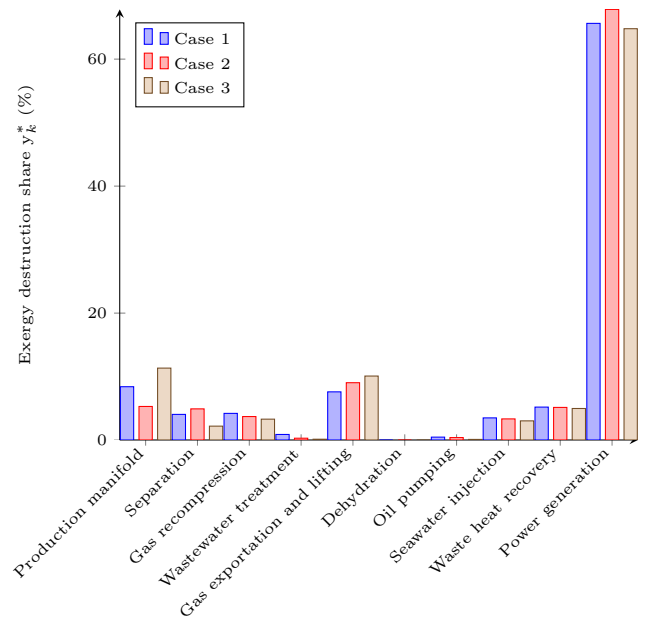
Figure 9: Exergy destruction share of the analysed simulation cases for an oil offshore platform

lifting process is in the same order of magnitude and is mainly due to the inefficiencies of the gas compressors (3.74-5.59 MW for the compressors alone).

The amount of exergy destruction is significantly greater in the case 3 than in the other cases, because of the higher content of gas in the well-fluid. This results in a larger flow rate to process in the production manifold and a higher volume of gas to compress to 15-20 MPa for exportation and lifting. Nearly equal exergy destruction takes place in the separation and re-compression steps, which is mainly due to the large inventory of mixers and recycles to enhance the hydrocarbon recovery. The smallest total exergy destruction of the process plant occurs in the case 2, where the crude oil fraction in the well-fluid is the largest and the water fraction the smallest of all studied cases. Although a larger flow rate is processed in the separation and pumping trains, which implies a higher amount of destroyed exergy in this sub-system, the exergy destruction in the production manifold is greatly reduced, which presents benefits at the scale of the overall processing plant.

Besides being responsible for large exergy destruction, the gas turbine system is also associated with large exergy losses, amounting from 15 to 18 MW, as shown in Table 10. The exergy losses are higher in the third case than in the two first ones because of the greater power demand of the process plant, which leads to a larger mass flow rate of flue gases and a higher stack temperature at the outlet of the waste heat recovery system.

Exergy losses associated with rejection of cooling water and wastewater overboard are comparatively small, since these streams are released at nearly atmospheric pressure and at a relatively close temperature to the ocean. Seemingly, exergy losses associated with flaring are negligible, since only gas ventilated from the glycol purification process is directly rejected into the environment without any valorisation. These losses increase with the amount of associated gas present in the well-fluid, as a larger gas flow rate leads to an increase in the amount of stripping gas required in the dehydration process, which is purged and discharged to the surroundings. The exergy losses in the investigated system total from 16.8 to 20.4 MW. About 90% of them is associated with rejection of high temperature exhaust gases to the environment. The remaining 10% is related to the exergy content of cooling and wastewater discharged overboard, as well as flared gases.

Table 10: Exergy losses (MW) of the analysed simulation cases for an oil offshore platform

	Case 1	Case 2	Case 3
Exhaust gases	15.5	17.3	18.7
Cooling water	1.1	1.4	1.3
Flared gases	0.21	0.25	0.33
Wastewater treatment	0.15	0.09	0.08
Total	16.8	19.0	20.4

Exergy efficiencies of the different sub-systems analysed in the baseline case are given in Table 11, with exergy rates expressed in MW. Since the production manifold, separation, and wastewater treatment consist mainly of throttles and mixers, the exergetic product is equal to null, which leads to the conclusion that the exergetic efficiency of these sub-processes is 0%.

Power generation and waste heat recovery are considered separately since they may be strongly dissimilar from platform to platform and since that they act as energy sources for the other processes. Exergy efficiency of this overall utility system is shown in Table 12, with exergy rates given in MW.

Table 11: Exergy efficiencies of the different process modules – Baseline Case

	Re-compression	Compression	Injection	Oil pumping
$\dot{E}_{d,k}$ (MW)	0.42	4.17	1.92	0.26
$\dot{E}_{f,k}$ (MW)	1.67	9.23	6.97	0.68
$\dot{E}_{p,k}$ (MW)	1.25	5.06	5.05	0.42
η_k (%)	74.8	54.8	72.4	61.7

Table 12: Exergy efficiency of the power generation and waste heat recovery system – Baseline Case

	Power Generation
$\dot{E}_{f,k}$ (MW)	85.7
$\dot{E}_{p,k}$ (MW)	26.4
η_k (%)	30.8

Results show that, apart from the production manifold and separation trains which are inherently exergetic-inefficient, the gas compression and the oil pumping sections have the lowest 2nd-law efficiency. However, the oil pumping section has a much smaller power demand, for both low and high gas-to-oil ratios, than the gas compression train. For this reason, concentrating efforts on improving the gas compression train may be more cost- and exergy-effective. Moreover, a higher efficiency of the gas compression train would result in a lower power consumption, decreasing thus the amount of exergy destroyed in the gas turbine systems.

6. Discussion

Process simulation results are in accordance with the findings of Svalheim et al. [2], who stated that the largest power demand corresponds to the gas compression step and may rise with time, as the gas-to-oil ratio may increase at the beginning of the life span of an oil field. Moreover, since the amount of produced water increases in any case, using wastewater from the crude oil separation process has become one of the focus of several studies from literature [14, 15, 20]. It is nevertheless emphasised that the hydrocarbon content of the wastewater emulsion may result in plugging issues, and therefore further research and quality control of the treated water are necessary.

Despite the differences in terms of process configurations and well-fluid composition with the work of Voldsund et al. [7, 8], the application of exergy analysis reveals that, in general, for North Sea oil platforms, the compression-lifting process is, when the utility system and the production manifold are not considered, the most exergy-destructive step, with a calculated exergy destruction rate of 4 to 6 MW. The main discrepancy lies in the accounting of the exergy associated with overboard discharge of cooling water, which is considered as an exergy loss in this study, but assumed as an exergy destruction in their work, due to differences in the choice of the system boundaries. Similarly, the re-compression and separation steps rank as the second and third most exergy-destructive sections, while the exergy destruction taking place in the oil export pumping is negligible.

The work of Voldsund et al. [7, 8] suggests to focus on the gas compression train. Improving this part of the offshore platform system is indeed of particular importance, since a more efficient gas process would lead to a reduction of the power consumption, and to a lower exergy destruction in the oil processing plant and in the power generation system. However, it should be added that operating the gas turbines in part-load mode is a key issue, and that therefore a compromise on the peak efficiency for a higher part-load efficiency may be beneficial over the life span of the oil field.

Oliveira and Van Hombeeck [6], who investigated a Brazilian oil platform, also emphasised the large exergy demand and destruction associated with the gas compression step. However, the authors pointed out the importance of the crude oil heating operations taking place before the separation module. The con-

siderable exergy consumption in the feed pre-heating is responsible for a furnace demand of about 25 MW exergy for a feed of 450 t/hr, which differs strongly from the findings of Voldsund et al. [7] and the present results. These discrepancies are mainly due to the temperature differences between the North Sea and the Brazilian feeds flowing out of the oil reservoir.

Oliveira and Van Hombeeck assumed feed characteristics of 7.4°C and 10.78 bars at the inlet of the separation train, whilst the well-fluid temperature is assumed here to 71°C at the inlet of the production manifold, which leads to a temperature of about 65°C at the inlet of the first-stage separator. These differences in results and conclusions suggest that oil offshore platforms located in different oil regions (North Sea, Gulf of Mexico, Brazilian Basin) may, with respect to exergy considerations, present highly different characteristics.

7. Conclusion

A generic North Sea offshore platform model was developed and presented, and predicts the material outflows and energy requirements under different sets of operating conditions and production flows. This overall model includes power generation, oil and gas processing, gas purification and seawater injection sub-models. The first sub-model was calibrated by use of published data from SIEMENS while the others were verified by comparison with open literature.

The performance of this integrated plant was assessed, based on the exergetic analysis method. Exergy is destroyed at a rate of 55-65 MW within the overall platform, with a share of 70-30% for the utility system (power generation and waste heat recovery) and the oil, gas and water processing, respectively. Exergy losses are also significant, amounting to about 17-20 MW, and are mostly due to the rejection of high-temperature exhaust gases from the cogeneration plant to the environment. However, the exergy destruction and loss rates represent only 0.5 to 1.5% of the total input exergy, due to the inherently large chemical exergy content of crude oil and natural gas.

Three simulation cases were investigated to analyse the effects of different gas-to-oil and water-to-oil ratios on the thermodynamic performance of this system, and to evaluate the exergy destruction share amongst the several system modules. The gas-to-oil ratio is the most important variable: a larger gas frac-

tion in the well-fluid stream causes a strong increase of the process plant power consumption and a larger exergy destruction in the production manifolds and gas compression trains.

Recovering more thermal exergy from the exhaust gases, improving the part-load efficiency of the gas turbine components and of the gas compression trains could significantly increase the thermodynamic performance of conventional oil and gas offshore platforms. Higher pressure levels in the separation train would lead to smaller exergy destruction rates in the manifold and re-compression trains, although this might result in a lower hydrocarbon recovery and conflict with the process constraints of other system sections.

Conventional exergy analysis does not allow evaluating interactions and cost flows between the system components and processes present on the whole offshore platform. Future work will address this issue by conducting an advanced exergy analysis, an exergoeconomic assessment and an evaluation of the uncertainties associated with the crude oil and gas compositions.

Acknowledgements

References

[1] Sentralbyrå, S.. Lavere klimagassutslipp i 2011 (in Norwegian). 2011. URL http://www.ssb.no/klimagassn_en/.

[2] Svalheim, S., Directorate, N.P., King, D.C., Exploration, B.P.. Life of Field Energy Performance. In: Offshore Europe. July; Aberdeen: Society of Petroleum Engineers Inc.; 2003, p. 5.

[3] Bothamley, M., Campbell, J.M.. Offshore Processing Options for Oil Platforms. In: SPE Annual Technical Conference and Exhibition. Houston; 2004, p. 1–17. doi: 10.2118/90325-MS.

[4] Bejan, Adrian; Tsatsaronis, George; Moran, M.. Thermal Design and Optimization. John Wiley & Sons, Inc.; 1995.

[5] Kotas, T.J.. The Exergy Method of Thermal Plant Analysis. London: Butterworths; 1985.

[6] Oliveira Jr., S.D., Van Hombeeck, M.. Exergy Analysis of Petroleum Separation Processes in Offshore Platforms. Energy Conversion and Management 1997;38(15-17):1577–1584.

[7] Voldsund, M., Ståle, I., Røsjorde, A., He, W., Kjelstrup, S.. Exergy Analysis of the Oil and Gas Separation Processes on a North Sea Oil Platform. In: Proceedings of ECOS 2010 - The 23rd International Conference on Efficiency, Cost, Optimization, Simulation and Environmental Impact of Energy Systems. Lausanne; 2010, p. 303–310.

[8] Voldsund, M., He, W., Røsjorde, A., Ertesvåg, I.S., Kjelstrup, S.. Evaluation of the Oil and Gas Processing at a Real Production day on a North Sea Oil Platform Using Exergy Analysis. In: Proceedings of ECOS 2012 - The 25th International Conference on Efficiency, Cost, Optimization, Simulation and Environmental Impact of Energy Systems. 2012, p. 260–274.

[9] Jones, D.S.J.. An introduction to crude oil and its processing. In: Handbook of Petroleum Processing; chap. 1. Springer; 2006, p. 1–45.

[10] Baker, R.O.N.. Oil and Natural Gas : Offshore Operations. 2004.

[11] Manning, F.S., Thompson, R.E.. OILFIELD PROCESSING OF PETROLEUM. Tulsa: PennWell Books; 1991.

[12] Plisga, W.C.L.G.J.. Standard Handbook of Petroleum & Natural Gas Engineering. Gulf Professional Publishing; second ed.; 2004. ISBN 0750677856.

[13] H. K., Abdel-Aal; M. A., Fahim; Mohamed, A.. Overview of Gas Field Processing. In: Petroleum and Gas Field Processing; chap. 10. New York: Marcel Dekker, Inc.; 2003, p. 1–6.

[14] H. K., Abdel-Aal, M. A., Fahim; Mohamed, A.. Produced Water Treatment. In: Petroleum and Gas Field Processing; chap. 9. Gulf Professional Publishing; 2003, p. 1–31.

[15] Vik, Eilan Arctander; Dinning, A.J.. Produced Water Re-Injection The Potential to Become an Improved Oil Recovery Method. Tech. Rep.; Aquatem A/S; Oslo; 2009.

[16] Abdel-Aal, H. K.; Aggour, Mohamed; Fahim, M.A.. Composition and Characteristics of Crude Petroleum - A brief review. In: Petroleum and Gas Field Processing; chap. 2. New York: Marcel Dekker, Inc.; 2003, p. 42–52.

[17] Ryba, A.. Optimization of Natural Gas Dehydration. Ph.D. thesis; AGH University of Science and Technology; 2005.

[18] Awal, M.R., Herd, B.L., Engineering, P.. Extent of Environmental Impact of Petroleum. In: Environmentally Conscious Petroleum Engineering; chap. 2. 2009, p. 12–15.

[19] Puntervold, T., Austad, T.. Injection of seawater and mixtures with produced water into North Sea chalk formation: Impact on wettability, scale formation and rock mechanics caused by fluid-rock interaction. In: Proceedings of SPE/EAGE Reservoir Characterization and Simulation Conference. Society of Petroleum Engineers; 2007, p. 1–12.

[20] Patton, C.C.. Injection-Water quality. Journal of Petroleum Technology 1990;42(10):1238–1240.

[21] SIEMENS, . SGT-500 Industrial Gas Turbine. Tech. Rep.; Siemens Industrial Turbomachinery AB; Finnspong; 2011.

[22] Song, T. W.; Kim, T. S.; Kim, J. H.; Ro, S.T.. Performance prediction of axial flow compressors using stage characteristics and simultaneous calculation of interstage parameters. In: Proceedings of the Institution of Mechanical Engineers. Institution of Mechanical Engineers; 2001, p. 89–98.

[23] Muir, D.E., Saravanamuttoo, H.I.H., Marshall, D.J.. Health Monitoring of Variable Geometry Gas Turbines for the Canadian Navy. Transactions of the ASME 1989;111(April):244–250.

[24] Spina, P.R.. Gas Turbine performance prediction by using generalized performance curves of compressor and turbine stages. In: Proceedings of the ASME Turbo Expo 2002. 2002, p. 1073–1082.

[25] Technology, A.. Aspen Plus - Modelling Petroleum Processes. Moutain View: Aspen Technology, Inc.; 1999.

[26] Technology, A.. Hysys 2004.2 Simulation Basis. Cambridge: Aspen Technology, Inc.; 2004.

[27] Dimian, A.C.. Integrated Design and Simulation of Chemical Processes. Amsterdam: Elsevier B.V.; first ed.; 2003. ISBN 0444829962.

[28] Elmegaard, B., Houbak, N.. DNA A General Energy System Simulation Tool. In: Proceedings of SIMS 2005 - 46th Conference on Simulation and Modeling. Trondheim: Tapir Academic Press; 2005, p. 1–10.

[29] Directorate, N.P.. Fact Pages. 2012. URL http://factpages.npd.no/factpages/.

[30] Szargut, J.. Chemical exergies of the elements. Applied Energy 1989;32(4):269–286.

[31] Morris, D.R., Szargut, J.. Standard chemical exergy of some elements and compounds on the planet earth. Energy 1986;11(8):733–755.

[32] Rivero, R., Rendon, C., Monroy, L., Group, E., Mexicano, I.. The Exergy of Crude Oil Mixtures and Petroleum Fractions: Calculation and Application. International Journal of Applied Thermodynamics 1999;2(3):115–123.